(4)

Nuclear Engineering and Design 56 (1980) 163–175

A MICROSTRUCTURE-DEPENDENT MODEL FOR FISSION PRODUCT GAS RELEASE AND SWELLING IN UO_2 FUEL *

M.J.F. NOTLEY and I.J. HASTINGS
Atomic Energy of Canada Limited, Chalk River Nuclear Laboratories, Chalk River, Ontario K0J 1J0, Canada

Received 17 March 1978

A model for the release of fission gas from irradiated UO_2 fuel is presented. It incorporates the relevant physical processes: fission gas diffusion, bubble and grain boundary movement, intergranular bubble formation and interlinkage. In addition, the model allows estimates of the extent of structural change and fuel swelling. In the latter, contributions of thermal expansion, densification, solid fission products, and gas bubbles are considered. When included in the ELESIM fuel performance code, the model yields predictions which are in good agreement with data from UO_2 fuel elements irradiated over a range of water-cooled reactor conditions: linear power outputs between 40 and 120 kW m^{-1}, burnups between 10 and 300 MW h(kg U)$^{-1}$, and power histories including constant, high-to-low and low-to-high power periods.

The predictions of the model are shown to be most sensitive to fuel power (temperature), the choice of diffusion coefficient for fission gas in UO_2, and burnup. The predictions are less sensitive to variables such as fuel restraint, initial grain size and the rate of grain growth.

1. Introduction

The release of fission product gas from UO_2 has been studied for many years; see, for example, Olander's recent review [1]. As yet, no single fundamental method of calculating release has been universally accepted, the major reasons being:

(i) many potentially important interacting variables are involved, the exact mathematical description of which can be complex;

(ii) the data against which hypotheses can be tested are themselves subject to considerable uncertainty, primarily due to uncertain fuel temperature histories; and

(iii) empirical release terms, based, for example, on apparent diffusion coefficient (D') calculations [2] or volume-averaged temperatures [3], have been correlated reasonably well with existing data, making the development of a rigorous fundamental model for steady-state operation less attractive.

However, to optimize fuel performance, there is an incentive to understand the role of factors such as element power (temperature), burnup, restraint and structure, on the amount of fission gas released. Also, since the activity of the released gas is an important consideration in accident analysis, a physically reasonable model which can include residence times for the various stages in the release process is desirable to facilitate extrapolation from the stable to the radioactive isotopes.

This paper describes a simplified model for calculating the release of stable fission-product gases from irradiated UO_2 fuel. The relevant physical processes are considered. The model takes an approach similar to that of Hargreaves and Collins [4], but extends their ideas to account for columnar as well as equiaxed grain growth, and considers the gas stored at the grain boundaries in more detail. In addition, the model allows an assessment of gas bubble swelling, including the effect of restraint on bubble size, and the effect of bubble volume on fuel thermal conductivity.

2. General description of gas release and swelling

Fuel temperature is the dominant parameter controlling fission gas release, as most of the pro-

* This paper is a revised or up-dated version of the paper actually presented at the IAEA Specialists' Meeting on Fuel Element Performance Computer Modelling.

Also, AECL-5838

cesses controlling gas atom movement in UO_2 are themselves temperature dependent. At low temperatures, gas atoms can be 'knocked out' or recoil from the fuel surfaces due to adjacent fission events. This effect, although important when considering the release of short-lived isotopes, is small when assessing the effects due to release of stable gases, and is not considered in the present paper.

In the generally accepted sequence of events leading to release, gas diffuses, either atomically or as bubbles, through the UO_2 grains. The size and distribution of the intragranular bubbles are controlled primarily by irradiation-induced resolution; their contribution to swelling is small. When the gas atoms arrive at the grain boundaries, they precipitate to form bubbles, which can grow until they interlink. Additionally, the bubbles, and the grain boundaries on which they are located, can also migrate, sweeping gas from the grains. Tunnels subsequently form at grain edges and gas ultimately escapes to voidage, such as fuel cracks or a plenum, within the element. After a period of high-power operation, it is postulated that gas is released from fuel during reactor shutdowns, because thermal shrinkage cracks follow or intersect the gas-filled tunnels or bubbles on the grain boundaries.

Fuel swelling originates from four main sources: positive effects due to thermal expansion, solid fission products and fission gas bubbles, and the negative effect due to densification. In this paper, we describe a model incorporating the gas release and swelling processes, show the sensitivity of the model to power, burnup, grain size, restraint and diffusion coefficient, and compare the predictions of the model with data from commercial and experimental water-reactor fuel.

3. Calculational procedure

3.1. Summary

The gas released during any constant power (temperature) period is calculated as follows:

(i) The fuel is divided into 100 annuli of equal thickness.

(ii) For each annulus a running inventory is kept of (*a*) gas produced in the annulus, (*b*) gas released from the grains in the annulus, and (*c*) gas stored in the intergranular bubbles. There is no transfer of gas from annulus to annulus.

(iii) Gas retained within the grains is assumed to diffuse to the boundary during the time interval, Δt, under consideration. At the start of the time interval, some fraction, f_0, of gas atoms has already been released from the grains. The effective time, t_0, to give the observed release, f_0, is first calculated from the appropriate diffusion equation for release from a sphere with zero production rate. The fractional release for the end of the time period is then calculated for time $t_0 + \Delta t$, and the number of atoms of gas released during the time period is obtained. The above procedure enables us to allow for time-varying diffusion coefficients such as result from a varying power history.

(iv) In addition to the gas present at the start of the time period (section iii), gas born within the grains during the time period is also available for release. The diffusion equations for release from a sphere with continuous generation of fission gas are used.

(v) The movement of grain boundary bubbles during the time period is calculated.

(vi) Grain boundary movements in the circumferential and axial directions, relative to the axis of the fuel elements, are assumed to be controlled by equiaxed grain growth; in the radial direction the boundary movement is assumed to be controlled by bubble movement, unless the rate of such movement is less than the rate due to equiaxed grain growth.

(vii) The number of grains per annulus and the corresponding grain boundary area are calculated.

(viii) A grain boundary accumulates gas as it 'sweeps' through the fuel.

(ix) The gas inventory at the boundary is stored in bubbles, with a maximum density of 6×10^{12} bubbles m^{-2} of grain boundary surface [5]. When the bubbles reach a size which allows them to interlink, any further gas arriving at the boundary is released to grain edge tunnels.

(x) The number of gas atoms stored in grain boundary bubbles is calculated, allowing for surface tension forces and external hydrostatic restraint from the element gas pressure and the fuel-to-sheath contact pressure.

(xi) Gas, once released to a grain edge tunnel, is available for release at a subsequent power change.

(xii) If the fuel melts, all the retained gas in the annulus is released, and the fuel solidifies from the melt with a grain size of 700 μm. The latter is not a critical assumption.

It should be noted that no account is taken of intragranular bubbles, or of re-solution of gas from a bubble into the matrix.

3.2. Diffusional release

Findlay [6] has measured the in-reactor diffusional release of ^{85}Kr from specimens of known surface-to-volume ratio. Use of this type of measurement enables us to calculate release from a sphere whether the gas migrates atomically or as intragranular bubbles. Findlay obtained a diffusion coefficient, D, given by:

$$D = 7.8 \times 10^{-2} \exp\left(-\frac{288 \text{ kJ mole}^{-1}}{R(T/10^3)}\right) \text{m}^2 \text{s}^{-1} \quad (1)$$

in which T is the absolute temperature and R the gas constant.

It has been suggested [7] that, at low temperatures, the diffusion rate is dependent on fission rate rather than temperature. We have therefore assumed, for normal water-cooled power reactor conditions, that the diffusion coefficient reaches a minimum limiting value at 1273 K.

When we calculate the gas release during a given time interval, Δt, we consider separately the gas born during the interval and that stored in the fuel up to the start of the time interval ('old' gas). Thus, for 'new' gas born during the time interval,

$$f = 4(Dt/a^2\pi)^{1/2} - 1.5Dt/a^2 \quad (2)$$

or, for

$$\pi^2 Dt/a^2 \geq 1,$$

$$f = 1 - \frac{a^2}{15Dt} + \frac{6a^2}{\pi^4 Dt} \exp\left(\frac{-\pi^2 Dt}{a^2}\right) \quad (3)$$

where f = the fractional release, D = diffusion coefficient, a = grain radius, and t = time interval.

When the fuel has an inventory of 'old' gas, and the release due to an additional time period or change in temperature is to be assessed, it is assumed that the fractional release at the start of the time period, f_0, was due to operation at the new conditions, and the time, t_0, to give the release, f_0, is calculated. We assume that the dynamics of 'old' and 'new' gas are independent, and for the 'old' gas, use the diffusion equations for zero production during the time step. Thus, t_0 is obtained from:

$$f_0 = 6(Dt_0/\pi a^2)^{1/2} - 3Dt_0 \quad (4)$$

which is valid for $\pi^2 Dt_0/\pi a^2 \leq 1$ or, if $\pi^2 Dt_0/a^2 \geq 1$,

$$f_0 = 1 - \frac{6}{\pi^2} \exp\left(-\frac{\pi^2 Dt_0}{a^2}\right). \quad (5)$$

The release of stored gas during the time interval Δt is obtained by calculating the release f_1 for time $t_1 = t_0 + \Delta t$, and subtracting the release up to time t_0. This additional gas release is added to that obtained previously from equation (2) or (3).

3.3. Equiaxed grain growth

Laboratory measurements of grain growth from various batches of UO_2 showed a significant difference between natural and enriched material, the most likely cause being differing impurity levels.

For natural UO_2, the grain growth is described by [8]:

$$d^{2.5} - d_0^{2.5} = 1.3 \times 10^6 \, t \exp\left(\frac{-320 \pm 10 \text{ kJ mole}^{-1}}{R(T/10^3)}\right) \quad (6)$$

and for enriched UO_2:

$$d^{2.5} - d_0^{2.5} = 1.7 \times 10^3 \, t \exp\left(\frac{-230 \pm 10 \text{ kJ mole}^{-1}}{R(T/10^3)}\right)$$

where d_0 = initial grain size (μm), d = final grain size (μm), t = time (s), T = temperature (K), and R = gas constant = 8.31 J mole^{-1} K^{-1}.

Section 4.5 evaluates the effect of changes in the assumed grain growth rates.

3.4. Grain boundary sweeping due to bubble movement

Bubble movement in a thermal gradient can occur by surface diffusion, volume diffusion or by vapour-phase transport [1]. Buescher and Meyer [9] summarize many of the observations and conclude that the rate of bubble movement is best approximated by taking a logarithmic average between the rates

for surface diffusion (V_s) and vapour phase transport (V_v). Accordingly we calculate, following Olander [1],

$$V_s = \frac{3D_s\delta Q_s^*}{RT^2 r_b}\frac{dT}{dx}\ \mathrm{m\ s^{-1}} \quad (8)$$

and

$$V_v = \left(\frac{4\times10^5\ \Omega}{kT}\right) D_g^* \left(\frac{T}{2000}\right)^{3/2}\left(\frac{0.1}{P}\right)\left(\frac{\Delta H_v}{RT}\right) \times \exp\left(\frac{\Delta S_v}{R}\right)\exp\left(-\frac{\Delta H_v}{RT}\right)\frac{1}{T}\left(\frac{dT}{dx}\right)\mathrm{m\ s^{-1}} \quad (9)$$

where D_s = surface self-diffusion coefficient [9]

$$5.4\times10\exp\left(\frac{-450\ \mathrm{kJ\ mole^{-1}}}{RT}\right)\ \mathrm{m^2\ s^{-1}},$$

δ = depth of surface diffusing layer = $\Omega^{1/3} = 3.4\times10^{-10}$ m,

Ω = molecular volume in solid = 4.1×10^{-29} m^3,

k = Boltzmann constant = 1.38×10^{-23} J K^{-1},

Q_s^* = surface diffusion heat of transport estimated at 450 kJ mole^{-1},

r_b = bubble radius (m),

dT/dx = temperature gradient (K m^{-1}),

D_g^* = diffusion coefficient for UO_2 vapour in Xe = 9×10^{-5} m^2 s^{-1} at 2000 K,

P = gas pressure within bubble (MPa),

ΔH_v = heat of vaporization = 567 kJ mole^{-1},

ΔS_v = entropy of vaporization = 150 J mole^{-1} K^{-1},

R = gas constant = 8.31 J mole^{-1} K^{-1},

$$V_{\mathrm{bubble}} = \exp[\ln V_s + \ln V_v)/2] = (V_s \times V_v)^{1/2}. \quad (10)$$

If the bubble velocity is lower than the velocity of the grain boundary due to equiaxed grain growth, then the boundary is assumed to move as if equiaxed growth was the driving force.

3.5. Effect of grain boundary sweeping on gas release

The fraction of the fuel volume swept by grain boundaries during a time period is calculated as follows. The grains are assumed to be cylinders of length L and diameter d, growing by amounts ΔL and Δd respectively. If the final number of grains in the annulus is n, then the unswept volume is $n(\pi/4)\,d^2L$. The swept fraction of the fuel volume, f_s, is thus given by:

$$f_s = \frac{n(\pi/4)(d+\Delta d)^2(L+\Delta L) - n(\pi/4)\,d^2L}{n(\pi/4)(d+\Delta d)^2(L+\Delta L)} \quad (11)$$

or

$$f_s = 1 - \frac{d^2L}{(d+\Delta d)^2(L+\Delta L)}. \quad (12)$$

When columnar grain growth becomes dominant, with the grain length very much greater than the diameter, sweeping is essentially unidirectional and due to bubble migration. We therefore must allow repeated sweeping of a given grain; this is done, as an approximation, by assuming that L in the above equation cannot exceed 200 μm. A better approach might allow sweeping to commence each time the bubble density at the cold end of the grain had reached a certain level.

The model tends to be self-compensating; if release by grain growth, and hence grain boundary sweeping, is reduced, more gas is released by diffusion, and vice versa.

3.6. Bubble size

A running inventory is kept of the number of gas atoms stored in the bubbles on the grain boundaries. We assume, based on post-irradiation measurements, that there is a maximum of 6×10^{12} bubbles m^{-2} of grain boundary surface [5]. The maximum bubble radius before interlinking is therefore about 2×10^{-7} m. The number of atoms, N, per unit of grain boundary is given by [1],

$$N = N_b\tfrac{4}{3}\pi r_b^2(2\gamma/kT)(1 + r_b\sigma/2\gamma) \quad (13)$$

where N_b = the number of bubbles per unit area,

r_b = bubble radius,

γ = the bubble surface tension,

k = the Boltzmann constant,

T = the temperature (K), and

σ = the hydrostatic stress acting on the bubble.

This equation is solved approximately for r_b, by incrementing r_b until $N_b = 6\times10^{12}$ m^{-2}.

The gas pressure in the bubble is calculated from

the number of atoms per bubble, and the pressure and bubble radius are used in the calculation of bubble velocity (§ 3.4). Note that all these calculations are 'steady state' and do not take into account the constraints on change in bubble size in a rapid transient, due, for example, to the creep of the surrounding UO_2.

3.7. Densification and swelling

Below about 1500 K the main contributions to volume change arise from irradiation-induced removal of sintering pores and accumulation of solid fission products (SFP). At higher temperatures, formation of fission gas bubbles becomes important. Superimposed on these effects is the influence of thermal expansion. Changes in porosity due to removal of sintering pores and gas bubble formation also affect fuel thermal conductivity.

Net densification is described by an empirical burnup- and temperature-dependent term fitted to data [10]

$$F = 0.6 - \exp[-(c_1 + c_2 T^3 B + c_3 T^3 B^2)] \qquad (14)$$

in which F is the fractional change in the volume originally occupied by sintering pores, resulting from irradiation-induced removal of pores plus accumulation of SFP, T is temperature (K), B is burnup MW h(kg U)$^{-1}$, $c_1 = 0.5064$, $c_2 = 2.038 \times 10^{-11}$ and $c_3 = -0.8186 \times 10^{-13}$. The remaining sintering pore volume is computed by allowing for the SFP swelling ($\Delta V/V$) which is assumed to be dependent on burnup and temperature (T) such that for $T < 1500$ K, $\Delta V/V = 1\%/240$ MW h (kg U)$^{-1}$ and for $T > 2200$ K, $\Delta V/V = 0.2\%/240$ MW h (kg U)$^{-1}$. Linear interpolation provides values of $\Delta V/V$ for $1500 < T < 2200$ K. Recent results from Zimmermann [11] support the concept of a temperature dependence in SFP swelling.

The fission gas bubble volume per annulus is computed from the numbers of gas atoms, the gas pressure and the annulus temperature. Intragranular gas bubbles are not considered; their swelling effect is negligible compared with that for intergranular bubbles [12,13].

3.8. Gas release from the grain boundary bubbles

When the bubbles are calculated to reach 2×10^{-7} m in radius, they are assumed to interlink. We define this as the point at which the boundary becomes saturated with gas atoms. When the grain boundaries become saturated, the additional gas that arrives during the time interval is released to grain edge tunnels [14]. We assume that gas is only released from the grain edge tunnels at a power change, with resultant fuel cracks opening a path to the interconnected voidage within the element. This 'step' release is observed in practice [15,16] especially with high-power fuel. This assumption makes no difference to the release computed for stable gases at end-of-life, but the assumption of a delay by trapping in the tunnels reduces the computed release of the radioactive species during constant power periods.

3.9. Transfer of gas atoms to grain boundary edge tunnels

The inventory of gas atoms present on the grain boundaries in each annulus changes as the grain boundary area per annulus changes or as fresh gas atoms arrive at the boundary. The ability of the boundary to retain these atoms depends on whether the bubbles have reached a size where they can interlink. The code is arranged so that at each time step the number of new atoms accumulated by a unit area of boundary, plus the old atoms remaining per unit grain boundary area from the previous time step, are compared with the maximum capacity of the boundary for retention of gas atoms. This defines the number of atoms retained per unit area of boundary, and hence the number of atoms retained on grain boundaries in each annulus. A running total is kept of the number of atoms released per annulus from the grains by diffusion or sweeping. The difference between this number and the number of atoms retained on the boundaries gives the release to the grain edge tunnels, and hence to the void volume within the fuel element.

4. Sensitivity studies

4.1. Effects of power and burnup

Fig. 1 illustrates the model predictions of fission gas release for a typical CANDU-PHW [1] fuel element

[1] CANada Deuterium Uranium-Pressurized Heavy Water

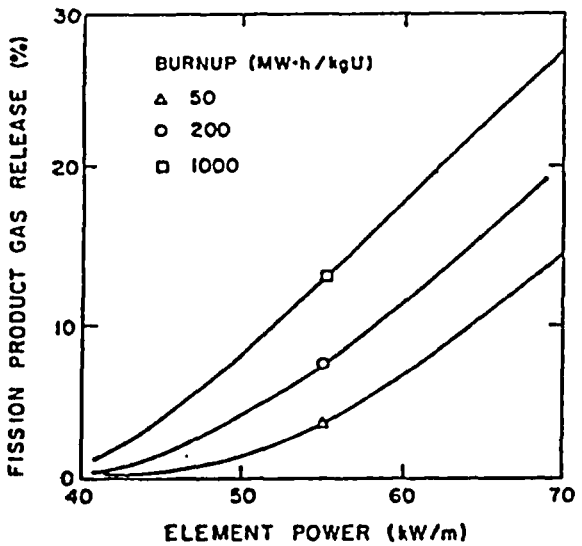

Fig. 1. Calculated dependence of fission-product gas release on element power and burnup. Surface temperature fixed at 675 K.

as a function of element power and burnup, with the surface temperature fixed at 675 K. Note that this is an artificial case to show parametric effects only; with a realistic history, release would be two or three times greater. The effect of power is clearly a major one. For example, from fig. 1, release is about 8% after 1000 MW h (kg U)$^{-1}$ at 50 KW m^{-1}; variation of ±10% on power results in corresponding releases of about 13 and 3%. The effect of ±10% variation in power on a calculated end-of-life temperature of 1750 K is ±150 K. In empirical relationships, fission gas release is commonly correlated against element power alone [17].

Fig. 1 also shows an increase in fractional gas release with burnup. The major factors influencing the increase are:

(i) gas is trapped at grain boundaries until the boundaries 'saturate', thus the volume of fuel able to release gas increases with time;

(ii) after the initial fuel densification, porosity due to fission gas bubbles reduces the thermal conductivity of the fuel, ultimately leading to higher fuel temperatures and gas release;

(iii) increased gas release leads to reduced fuel-to-sheath heat transfer and higher fuel temperatures; and

(iv) a time dependence is inherent in the Booth formalism for diffusion [18].

At 60 KW m^{-1}, the gas release is 8 and 12% at 50 and 300 MW h (kg U)$^{-1}$ respectively. Thus for burnups within our current experience (≤ 300 MW h (kg U)$^{-1}$) the increase is small enough that it could equally be due to a 10% uncertainty in element power. It will be difficult therefore to test the model predictions by experiment; a long period of steady reactor power is required.

Speculation on extending the model predictions to high burnups is contained in § 6.

4.2. Initial grain size

Initial grain sizes of about 10 μm are common in commercial UO_2 fuel. There is experimental evidence that increasing the starting grain size up to 100 μm can reduce fission gas release and swelling [19,20]. Fig. 2 shows the predicted effect of initial grain sizes varying from 10 to 50 μm on fission gas release, as a function of burnup and power for an artificial history. A reduced fission gas release with increasing initial grain size is shown. For example after 1000 MW h (kg U)$^{-1}$ at 50 kW m^{-1}, gas release are about 4 and 8% for initial grain sizes of 50 and 10 μm respectively.

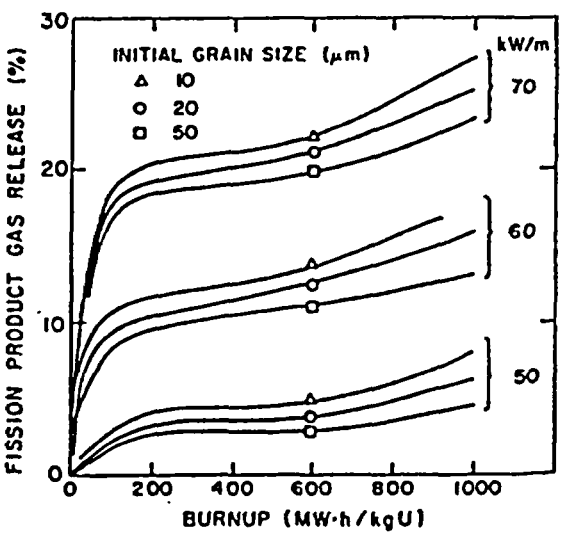

Fig. 2. Effect of initial grain size on fission gas release at a range of element powers. Fuel surface temperature is fixed at 675 K.

At low powers, the model indicates that both gas migration due to diffusion and the fractional amount of fuel swept by grain boundaries will be reduced by a large initial grain size, leading to lower gas release. A compensating factor is that the inventory of gas stored on the boundaries is a function of grain boundary surface area; thus for large grains, less gas is stored and more of the arriving gas is available for release. At higher powers, where columnar grain growth is responsible for most of the gas release, initial grain size has a reduced effect on release. The results suggest that a stable initial grain size larger than the maximum grain size predicted for the irradiation conditions would be most effective in reducing gas release.

The model also predicts reduced fuel swelling with increasing initial grain size. After 1000 MW h (kg U)$^{-1}$ at 50 KW m^{-1}, the maximum local fuel volume change for an initial grain size of 10 μm is about 11%; for an initial grain size of 50 μm, the change is about 7%. We do not yet have data to check these predictions.

4.3. Hydrostatic restraint

The amount of gas retained at the grain boundaries is a function of the gas pressure within the bubbles. At the time of interlinkage, the model assumes the bubble diameter to be 4×10^{-7} m, at which size the surface-tension-induced gas pressure is about 35 MPa at 1600 K. In a CANDU fuel element, internal gas pressures can be of the same magnitude as the coolant pressure (10 MPa). In addition there is a component due to fuel-to-sheath contact so the hydrostatic restraint or stress state in the UO_2 around the bubble is significant. At steady power, we would expect an equilibrium to be set up in which the swelling rate caused by the growth of gas bubbles just balances the outward creep of the sheath.

It has been argued that changes in hydrostatic restraint can cause changes in bubble volume [21]. Deductions of the fuel-to-sheath gap width based on measurements of the heat transfer coefficient were interpreted as showing that the fuel pellet shrank when the internal gas pressure in the element was raised, and the pellet increased in diameter when the pressure was lowered. Further qualitative support of the effect of hydrostatic restraint is found in an examination of a UO_2 fuel element irradiated in organic coolant [22]. The swelling of UO_2 clad in heat-treated Zr-2.5 wt% Nb alloy was significantly less in the braze-affected areas of the cladding compared with that in the adjacent areas which exhibited lower creep strength. The possible effects of hydrostatic restraint are discussed further in § 5.1.

4.4. Diffusion coefficient

Fig. 3 shows the effect of varying the fission gas diffusion coefficient by a factor of five, as a function of element power and burnup for an artificial history. The fractional change in fission product gas release is less at high element powers since at high powers grain boundary sweeping is releasing a large fraction of the fission gas. The effect of the factor of five change in diffusion coefficient is about the same as that of a 10% uncertainty in element power, or ±200 K for a fuel temperature of 2000 K.

4.5. Rate of grain growth

The effect on fission gas release of varying the rate of grain growth by a factor of five is shown in

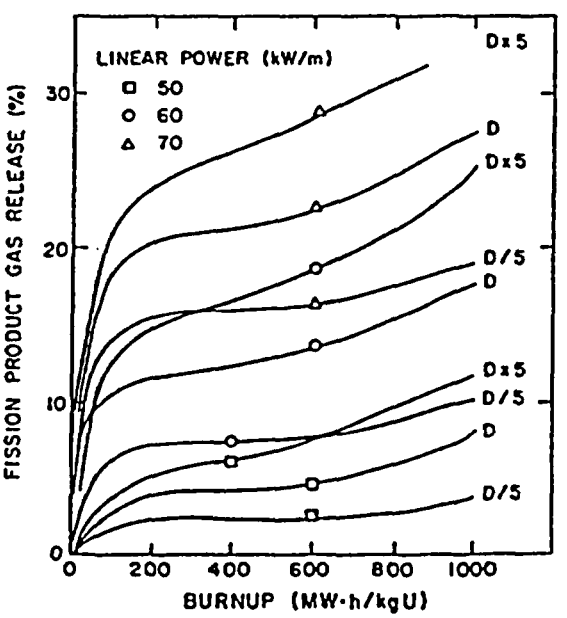

Fig. 3. Effect of varying gas diffusion coefficient D by a factor of five, for a range of powers. Fuel surface temperature is fixed at 675 K.

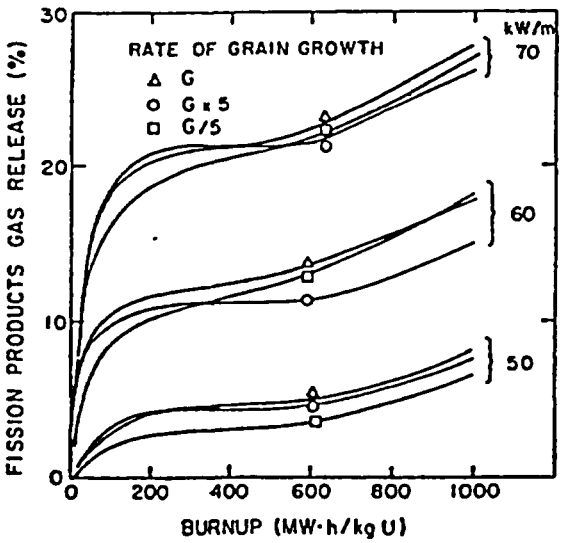

Fig. 4. Effect of varying rate of grain growth G by a factor of five, for a range of powers. Fuel surface temperature is fixed at 675 K.

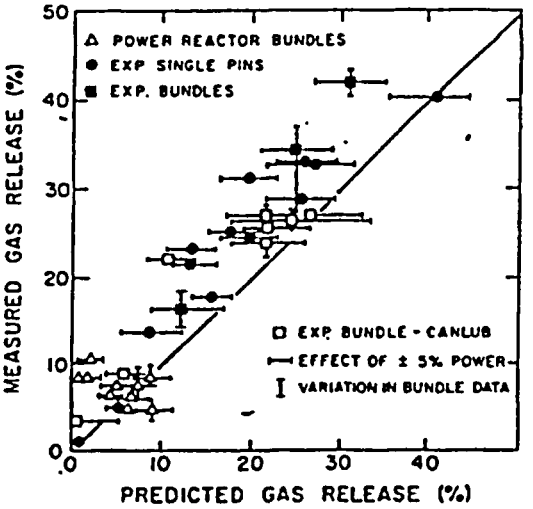

Fig. 5. Measured fission product gas release compared with predictions of ELESIM without modification. Line represents perfect agreement.

fig. 4 for an artificial history. The effect is significantly less than that due to varying the diffusion coefficient, for example. The results lie within the evelope due to ±5% uncertainty in fuel power. At the highest grain growth rate, fractional release is initially increased due to the gas-collecting effect of boundary sweeping. However, as grains grow, release is reduced as diffusion distances increase.

The grain growth rate at 1800 K in natural UO_2 (eq. 6) is only about 30–40% greater than that for enriched UO_2 (eq. 7). The relative insensitivity to grain growth rate thus indicates that the grain growth equation is not a critical factor in gas release, though obviously important in structure prediction. However, note from § 4.2 the significance of a large initial grain size.

5. Comparison with experiment

5.1. Fission product gas release

Fig. 5 shows that the model, incorporated into the ELESIM fuel performance code [23], gives predictions of fission gas release in reasonable agreement with a wide variety of experimental data. Results are presented from experimental and commercial fuel irradiated to burnups between 10 and 300 MW h $(kg\ U)^{-1}$, with powers between 40 and 120 kW m^{-1} [24]. The fuel histories considered include constant power, low-to-high power, high-to-low power periods, and combinations of these. No systematic deviation, either with burnup or element power, is observed. However, there is a tendency to underpredict, equivalent to a change of about 5% in element power output. Since the model was to be used in a design code, it was modified to increase gas release, so that measured and predicted release were, on average, equivalent. This was done by arbitrarily increasing the diffusion coefficient by a factor of three, as shown in fig. 6; the modified diffusion coefficient is still within the scatter evident in Findlay's [6] data. This tuning has the desired effect, as shown in fig. 7.

A more severe test is to compare model predictions with observations of dynamic release during a power transient. This type of comparison evaluates the time-response characteristics of the model. A reasonable correlation is required if the model is to be used for radioactive species, which decay appreciably in the time interval before they are released, or for extrapolation to transients occurring during loss-of-coolant accidents.

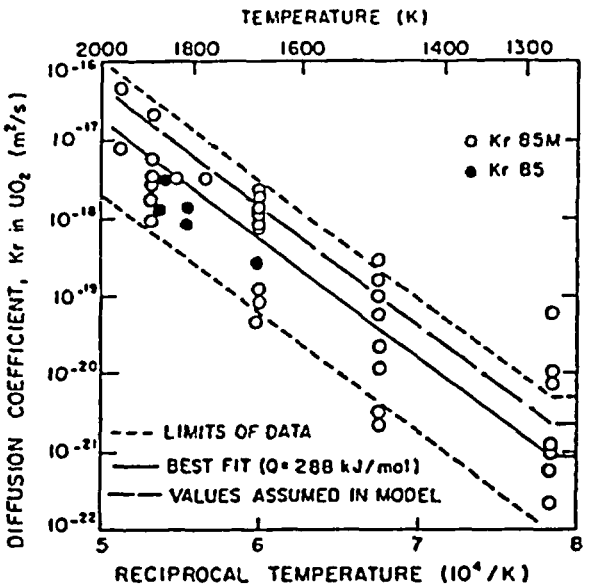

Fig. 6. Diffusion coefficient for ^{85}Kr in UO_2 under irradiation showing limits and best fit to data, and values assumed to modify gas release model.

There is only one test with the relevant information. Campbell et al [16] ramped two stainless-steel-sheathed UO_2 fuel elements from 50 to 70 kW m^{-1} after 105 MW h (kg U)$^{-1}$ and measured the gas

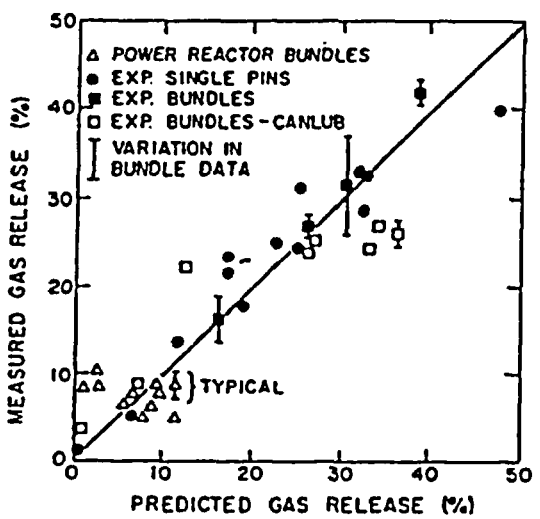

Fig. 7. Measured fission product gas release compared with predictions of ELESIM with the diffusion coefficient increased by a factor of three, as shown in fig. 6. Line represents perfect agreement.

release during the subsequent 5.2 X 10^6 s using gas-pressure sensors. Comparison with the prediction of the modified model is shown in fig. 8; where it is apparent that gas is released much faster than the model predicts. One possible cause of the anomaly can be examined quantititatively. If the fuel-to-sheath interfacial pressure is kept constant at 0.1 MPa, about that at the start of the ramp, agreement is much better, as shown by the solid line in fig. 8. This implies that the stresses imposed on the surface of the UO_2 pellet by the strained sheath were not transmitted to the central regions of the pellet; the load was thus supported by the bridging annulus. With lower hydrostatic stresses in the UO_2, less gas is retained on 'saturated' grain boundaries. An alternative explanation stems from the observation that the measured grain size at the end of the irradiation was about a factor of ten greater than the 85 μm predicted. It is unlikely that powers were greatly in error, so we suspect that the cause of the discrepancy may be a high O/U ratio at the center of the fuel before the power boost. This would have caused enhanced grain growth and gas release, and might occur because of redistribution of oxygen in the thermal gradient. This should only be important for stainless-steel-sheathed elements, since for Zircaloy-sheathed elements, the fuel composition approaches stoichiometry because of the oxidation of the Zircaloy. Further tests are required to test the response of the model to transient conditions.

5.2. Swelling

Hastings and Rose [25] have measured the local density changes in commercial UO_2 fuel after about 200 MW h (kg U)$^{-1}$. Fig. 9 compares their measurements from one element with predictions of the model. Maximum calculated central temperature was 2150 K; maximum surface temperature was 670 K. Agreement is reasonably good; further details are given elsewhere [26]. In particular, the magnitude and radial position of the observed swelling peak is in fair agreement with prediction, giving further credence to the model. Note that agreement in the densifying region at fractional radius >0.7 is expected because of the empirical fit employed. Measured results lie within the envelope due to ±5% uncertainty in operating power.

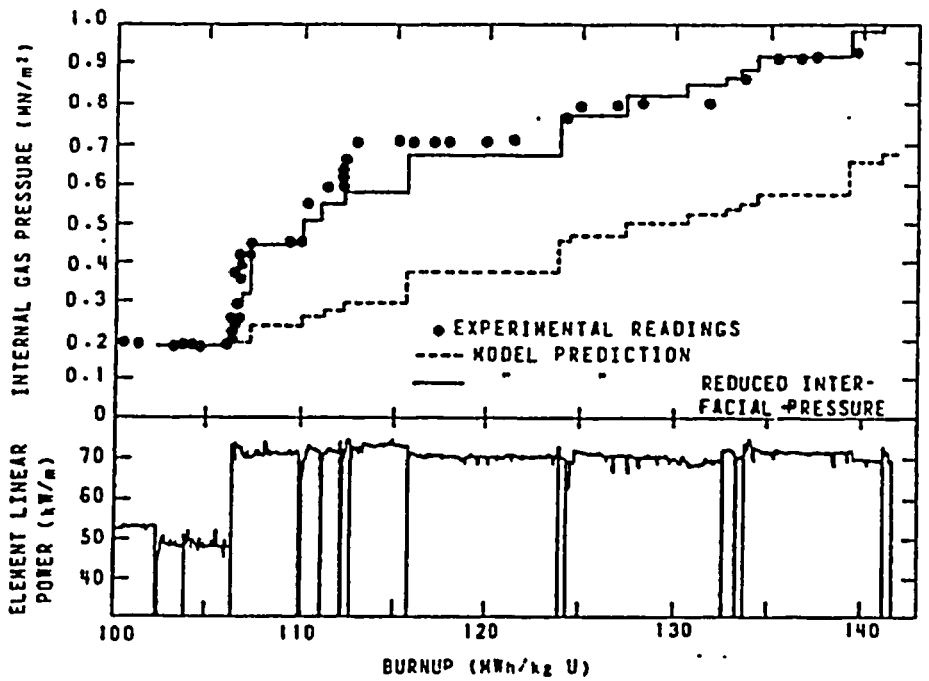

Fig. 8. Comparison of measured and predicted gas releases for a test [16] in which a fuel element was power ramped after 106 MW h (kg U)$^{-1}$ burnup.

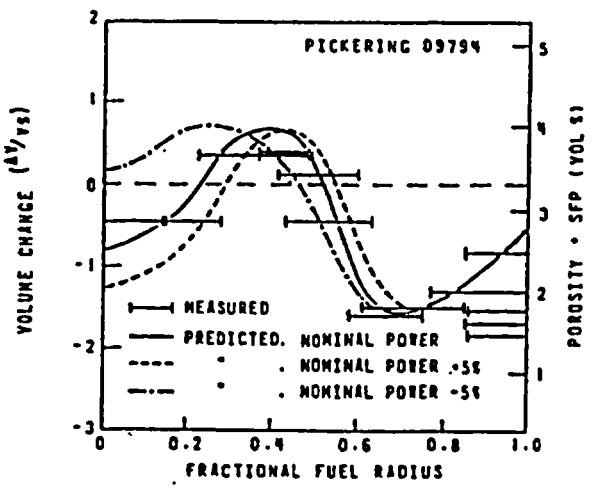

Fig. 9. Comparison of measured (bars) and predicted (solid line) volume changes as a function of fractional fuel radius, for a Pickering element after about 200 MW h (kg U)$^{-1}$ [26]. Values for nominal power ±5% are also given.

5.3. Fuel structural change

Comparisons of the predicted radial extent of fuel structural changes with experimental data are shown in fig. 10. Data on equiaxed and columnar grain growth, plus limits of melting are included. The details of the element power histories used in these simulations are given elsewhere [24]. Agreement is reasonable, within about ±10% uncertainty in element power.

Fig. 11 (from Hastings et al. [8]) presents predicted and observed equiaxed grain sizes in commercial fuel. Agreement is good up to a measured grain size of about 40 μm after which overprediction occurs. All results lie within the envelope due to ±5% variation in nominal element power. MacEwan and Hayashi [27] and Ainscough et al [28] suggested that grain growth is inhibited by irradiation. However, an inhibition algorithm is not included in the current model, since any inhibition effect is comparable with the ±5% uncertainty in the power history

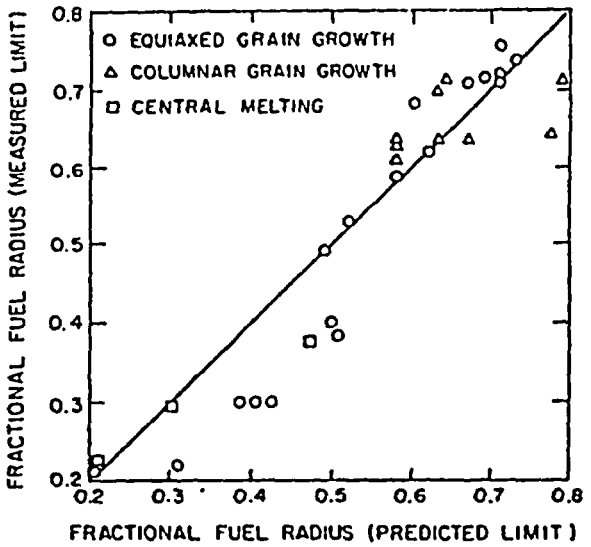

Fig. 10. Measured versus predicted radial extent of structural change in UO_2 fuel elements. Line represents perfect agreement.

data. Note also, from the sensitivity studies in §4.5, that grain growth variation in the range shown in fig. 11 would not significantly affect fission gas release.

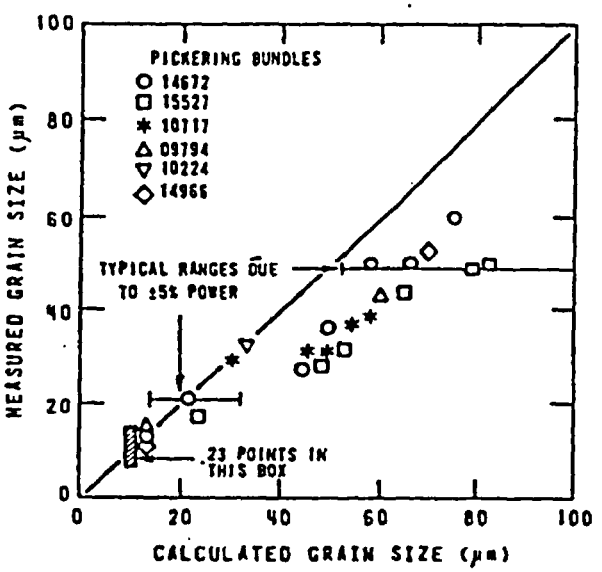

Fig. 11. Observed versus predicted grain sizes in UO_2 after Hastings et al. [8]. Nominal power histories used in all cases. Line represents perfect agreement.

6. Extrapolation to high burnup conditions

There is strong evidence that fractional gas release is enhanced at burnups $\geq$500 MW h (kg U)$^{-1}$. For example, recent data from the Zorita reactor [29] show fractional gas release increasing with burnup between 700 and 1300 MW h (kg U)$^{-1}$.

Fig. 1 shows that an increase in fractional release with burnup is predicted by the model. Fig. 12 attempts to illustrate the reasons for such an enhancement. The plot is for a PHW fuel element, typical except for a large plenum and helium filling gas. Curve (A) illustrates the burnup dependence at 50 kW m^{-1} if fuel surface temperature and fuel thermal conductivity are held constant. Curve (B) shows the effect of allowing for the helium filling gas. Initially, the improved fuel-sheath heat transfer due to the filling gas results in temperatures, and thus gas release, lower than (A). Subsequent dilution of the filling gas, and increase in internal pressure due to released fission products, reduces the fuel-sheath

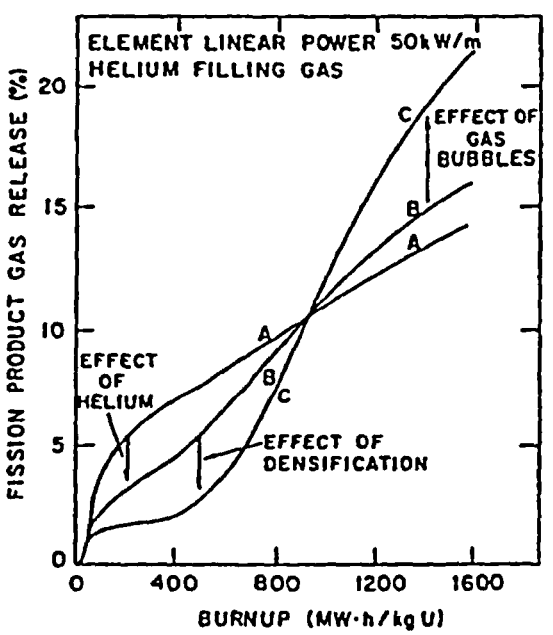

Fig. 12. The predicted fission-product gas release from a UO_2 fuel element (A) keeping fuel porosity and temperature constant, (B) variable fuel surface temperatures with constant porosity and (C) variable fuel surface temperatures and porosity (fuel thermal conductivity).

heat transfer coefficient resulting in temperatures and gas release higher than for (A) at burnups above about 1000 MW h (kg U)$^{-1}$. In curve (C), fuel densification and fission gas bubbles affect fuel conductivity, in addition to the effect of helium and internal gas pressure on fuel-sheath heat transfer. Initial densification increases fuel conductivity, thus reducing temperatures and fission gas release compared with (B). The effect of subsequent fission gas bubble growth on fuel thermal conductivity is the primary cause of the upswing in release above (B) at burnups greater than 1000 MW h (kg U)$^{-1}$.

Although there may be other phenomena contributing to gas release at very high burnups, such as the creation and movement of significant intragranular porosity, it is encouraging that our existing simple model can account qualitatively for the tendency towards higher release at a burnup above about 1000 MW h (kg U)$^{-1}$.

7. Conclusions

We have described a simplified model for fission gas release from UO_2 incorporating diffusion, grain boundary movement and the accumulation and interlinkage of bubbles at grain boundaries. The model gives results in reasonable agreement with experimental fission gas release data from UO_2 fuel elements irradiated under a range of PHW reactor conditions: linear powers between 40 and 120 kW m^{-1}, burnups of 10 to 300 MW h (kg U)$^{-1}$ and histories including constant, high-to-low and low-to-high power periods. The model predicts a tendency to higher gas releases for fuel irradiated to burnups above 1000 MW h (kg U)$^{-1}$.

The model also yields estimates of fuel swelling and extent of structural change which are in reasonable agreement with observed data.

The predictions of the model are shown to be most sensitive to fuel power (temperature), diffusion coefficient for fission gas in UO_2, and burnup. The predictions are less sensitive to variables such as fuel restraint, initial grain size and the rate of grain growth.

Acknowledgement

The cooperation of Ontario Hydro in providing irradiated fuel from their commercial reactors is gratefully acknowledged.

References

[1] Donald R. Olander, Fundamental Aspects of Nuclear Reactor Fuel Elements, ERDA Report TID 26711 (1976).
[2] W.B. Lewis, Atomic Energy of Canada Limited, Report AECL-1402 (1961).
[3] J.P. Hoffman and D.H. Coplin, General Electric (US) Report GEAP-4596 (1964).
[4] R. Hargreaves and D.A. Collins, J. Brit. Nucl. Energy Soc. 15 (1976) 311.
[5] I.J. Hastings, CRNL, Unpublished work.
[6] J.R. Findlay, BNES Conference Chemical Nuclear Data, Canterbury U.K. (1971).
[7] Hj. Matzke, Physics of Ionized Gases, Proc. Int. Summer School, Herceg-Novi, Ed. B. Navinsek, Ljubljana (1970) 374.
[8] I.J. Hastings, J.A. Scoberg and Kathy Mackenzie, Grain Growth in UO_2: In-Reactor and Laboratory Testing, J. Nucl. Mater. to be published. Also Atomic Energy of Canada Limited, Report AECL-6411 (1979).
[9] B.J. Buescher and R.O. Meyer, J. Nucl. Mater. 48 (1973) 143.
[10] I.J. Hastings and L.E. Evans, J. Am. Ceram. Soc. 62, 3–4 (1979) 217.
[11] H. Zimmermann, Institut für Material- und Festkorperforschung, Karlsruhe, KFK 2467 (1977).
[12] R.M. Cornell, J. Nucl. Mater. 38 (1971) 319.
[13] I.J. Hastings, Atomic Energy of Canada Limited, Report AECL-4942 (1974).
[14] J.A. Turnbull and M.O. Tucker, Phil. Mag. 30 (1974) 47.
[15] M.J.F. Notley, R. Deshaies and J.R. MacEwan, Atomic Energy of Canada Limited, Report AECL-2662 (1966).
[16] F.R. Campbell, R. Deshaies and M.J.F. Notley, Atomic Energy of Canada Limited, Report AECL-4912 (1974).
[17] J.R. MacEwan, A.S. Bain, M.J.F. Notley and R.W. Jones, Proc. 4th Int. Conf. Peaceful Uses of Atomic Energy, Vol. 10. (U.N., N.Y., 1971) 245.
[18] A.H. Booth, Atomic Energy of Canada Limited, Report AECL-496 (1957).
[19] R.D. MacDonald, Atomic Energy of Canada Limited, Report AECL-1810 (1963).
[20] J.A. Turnbull, J. Nucl. Mater. 50 (1974) 62.
[21] M.J.F. Notley, F.R. Campbell, I.J. Hastings and H.E. Sills, ANS Topical Meeting Water Reactor Fuel Performance (St. Charles, Ill., May, 1977) 114–122. Also Atomic Energy of Canada Limited, Report AECL-5787 (1977).

[22] I.J. Hastings and M.H. Schankula, J. Nucl. Mater. 61 (1976) 229.
[23] M.J.F. Notley, Nucl. App. and Tech. 9 (1970) 195.
[24] Kathy Mackenzie, Atomic Energy of Canada Limited, Private Communication.
[25] I.J. Hastings and D.H. Rose, Irradiation-Induced Volume Changes in Pickering Fuel, Annual Meeting, Am. Ceram. Soc., Cincinnati, Ohio (April 1976).
[26] I.J. Hastings, M.J.F. Notley and D.H. Rose, J. Nucl. Mater. 75 (1978) 301.
[27] J.R. MacEwan and J. Hayashi, Proc. Brit. Ceram. Soc. 7 (1967) 245.
[28] J.B. Ainscough, B.W. Oldfield and J.O. Ware, J. Nucl. Mater. 49 (1973/74) 117.
[29] E. Roberts, M.G. Balfour, G.W. Hopkins, W.R. Smalley and E. Dequidt, ANS Topical Meeting Water Reactor Fuel Performance (St. Charles, Ill., May, 1977) 133–146.